

Environmental Changes caused by COVID-19 and the Associated Societal Responses: A Review

**Deepali Mishra
Data Scientist [AI, GIS]**

HIGHLIGHTS

- Changes in Air quality
- Wildfire events
- Deforestation
- Urban growth

Abstract

This study entailed a review of environmental changes caused by COVID-19 and the associated societal responses. The topic itself describes the effect of COVID-19 on Air quality, Deforestation, Wildfires & urbanization. It includes the use case of both statistical data and satellite data for getting the impact of the COVID-19 pandemic. Understanding the spatiotemporal dynamics of COVID-19 is essential for its mitigation, as it helps to clarify the extent and impact of the pandemic and can aid decision-making, planning, and community action. This review concludes that to fight COVID-19, it is important to face the challenges from an interdisciplinary perspective, with proactive planning, international solidarity, and a global perspective. This review provides useful information and insight that can support future bibliographic queries, and also serves as a resource for understanding the evolution of tools used in the management of this major global pandemic of the 21 Century.

Introduction

Approximately 2 years have passed since Chinese authorities identified a deadly new coronavirus strain, SARS-CoV-2 (January 7, 2020); four months since the WHO declared a pandemic (March 11, 2020). This report focuses on the environmental changes caused by COVID-19 and the associated societal responses. Various empirical studies have been conducted into the COVID-19 pandemic effect on the environment. These studies have consistently found that the visual and interactive aspects of the COVID-19 on environment and society are somewhere worse for humanity and somewhere it turns blessing for the environment.

The geographic distribution of COVID-19 cases (Figure 1), and the epidemic curve indicating the number of confirmed cases and deaths in different parts of the world are illustrated in Figure 2. These are the updated information up to 06 September 2020.

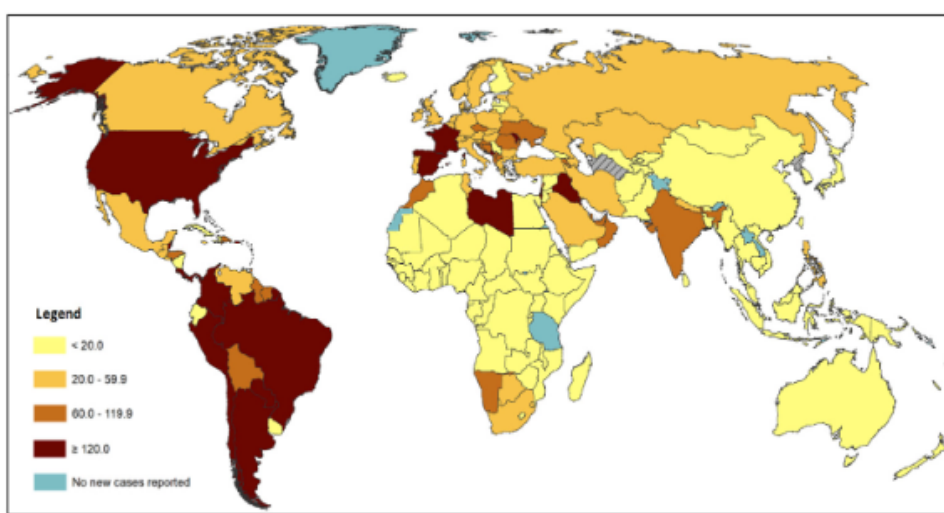


Figure 1. Geographic distribution of the 14-day cumulative number of reported COVID-19 cases per 100000 populations, as of September 06, 2020 (Source: ECDC, 2020).

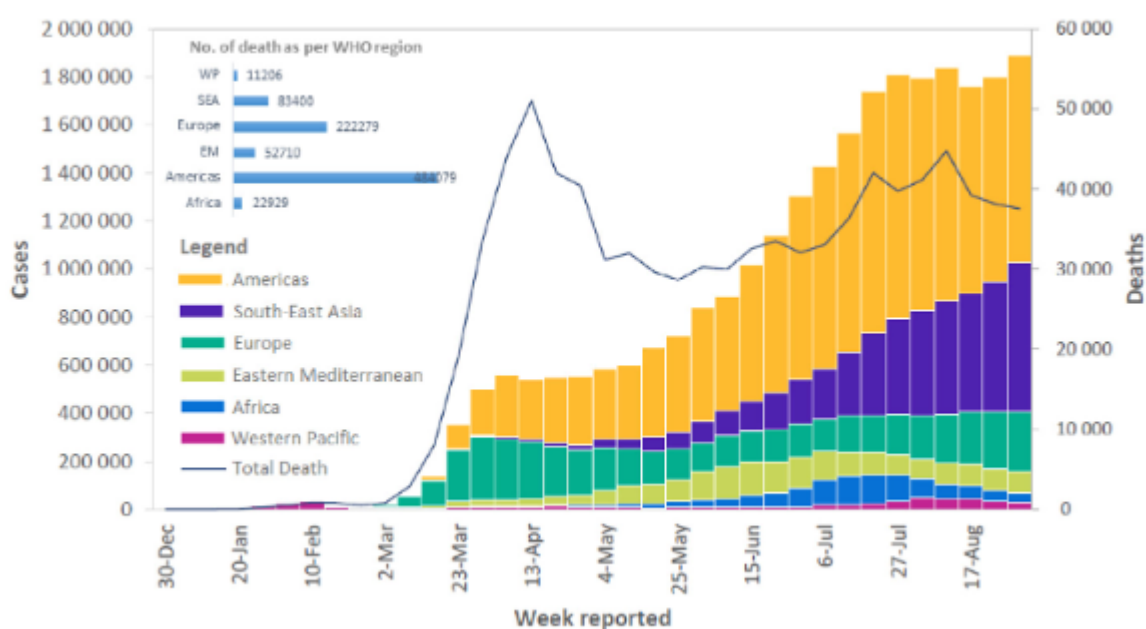


Figure 2. Number of COVID-19 cases reported weekly by WHO region, and total deaths, up to September 06, 2020 (Data source: WHO, 2020c).

This study around environmental changes has been performed by reviewing the available satellite data, case studies, and different government and non-government organizations' information from reports and official websites. Satellite data has been collected through Copernicus Hub/ USGS Earth Explorer. It includes the study of vegetation indices, AQI (Air Quality Index), Built-up index, burnt index. A large number of studies present the data and information which are relevant to the environmental effects of COVID-19.

Environmental effects of COVID-19

1. Changes in Air Quality

While the socio-economic devastation due to COVID-19 has been colossal around the world, which required "a wartime" plan from every corner of the world it has also come as the silver lining for the environment. The United Nations Environment Program chief Inger Andersen believes these environmental changes are temporary, as the global environment had a small respite before industrial activities resumed since February 2020. Recent studies have reported improvement in air quality due to restrictions placed upon industrial activities during the lockdown. Climate scientists have indicated that greenhouse gaseous (GHGs) concentrations could drop to levels not seen since World War II. Highly industrialized cities located in cold climate zones observed a higher reduction in air pollution. Lockdown in various countries viz., France, Germany, Italy, Spain, and China led to shutting down of power plants, transportation, and other industries which resulted in a drastic decrease in concentration levels of GHGs, NO₂, PM_{2.5}, PM₁₀, and CO but spikes in ozone concentration simultaneously, primarily in Europe and large Chinese cities. The air quality changes during COVID-19 lockdown over the Yangtze River Delta Region suggest that the reduced human activity and industrial operations lead to a significant reduction in PM_{2.5}, NO₂, and SO₂. Significant improvement in air quality, as evidenced from the reduction in Particulate Matter, NO₂, SO₂, and CO, during the COVID19 lockdown period was observed in the Hangzhou megacity. Reduction of NO₂ (49%) and CO (37%) concentrations in the USA during lockdown were positively correlated with higher population density. The impact of the measures on the air quality is discussed for the city of Rio de Janeiro, Brazil by comparing the particulate matter, carbon monoxide, nitrogen dioxide, and ozone concentrations during the partial lockdown with those of the same period of 2019 and also with the weeks prior to the virus outbreak. The positive impact of the social distancing measures is reported¹⁷ on the concentrations of the three main primary air pollutants (PM₁₀, NO₂, and CO) of the São Paulo and Rio the Janeiro, the two most populated cities, wherein, the CO levels showed the most significant reductions (up to 100%) which was related to light-duty vehicular emissions. Changes in levels of some air pollutants due to a set of rapid and strict countermeasures limiting population's mobility and prohibiting almost all avoidable activities were evaluated in Salé city (North-Western Morocco). Barcelona city was assessed¹⁹ for air quality using a remote sensing dataset provided by ESA's Tropospheric monitoring instrument (TROPOMI) along with local air quality monitoring data to assess differences in air quality during the lockdown and one month before the lockdown. The observed reductions were 31% and 51% in NO₂ and PM_{2.5}, respectively, due to lockdown. The National Aeronautics and Space Agency (NASA), using the TROPOMI sensor, observed a reduction of 10–30% in Nitrogen Dioxide (NO₂) in central and eastern China during early 2020. 27% reduction was observed in nitrogen oxides concentration in comparison to the last five years, and non-uniform trends in O₃ concentrations during the lockdown in the California basin region. Black carbon reduction due to the lockdown imposed restricted anthropogenic activities is observed in Hangzhou city of China. A reduction of 43% and 31% in PM₁₀ and PM_{2.5}, while a 17% increment in O₃ concentration during the lockdown period and past 4-year values for different regions of India has also been reported.

The common air pollutants in cities and industrial towns are NO₂, SO₂, PM10, which are responsible for cardiovascular and respiratory diseases. The primary sources of these pollutants are vehicular exhaust, road dust, and mainly metal processing industries. The majority of the health benefits were observed with the reduction in NO₂ in provincial capital cities in China. Continuous degradation of air quality in some of the Indian metropolitan cities (New Delhi, Mumbai, Kolkata, Chennai), that often exceeds the standards set by WHO and Central Pollution Control Board (CPCB). India cemented their regular presence in the list of top 20 polluted cities of the world. The Ministry of Earth, Forest, and Climate change (MoEFC) under its National Clean Air Programme (NCAP) launched a five-year action plan in 2019 to reduce by 30% the nationwide concentration of particulate matter. Due to the mandatory lockdown imposed across the country, 88 Indian cities have observed a drastic reduction in air pollution.

Gujarat, which is the industrial state in western India, observed a significant reduction in major air pollutants between the lockdown period (March 25 to April 20, 2020) mainly due to restrictions on traffic and slowdown of production at factories. According to the CPCB-AQI database, air pollution reduction occurred merely in four days since the lockdown.

1.1. Study-Area

Ankleshwar is located at 21.62°N, 73.01°E is a municipality under Bharuch district jurisdiction in Gujarat, India (Figure 3). It is located in the south Gujarat region in between the Ahmedabad—Mumbai industrial corridor on the southern banks of the lower reaches of the Narmada River. The city has plain topography with an average elevation of 15 m above mean sea level. The climate of the South Gujarat region is mainly influenced by the Arabian Sea. Pre-monsoon showers announce the arrival of monsoon only in late June, with hot summer months (March to June), heavy to moderate monsoon rain (July to September), and moderate winter months (November to February). Ankleshwar Gujarat Industrial Development Corporation is spread over an area of 1600 hectares and houses more than 2000 industries with over 1500 chemical plants producing pharmaceuticals, paints, and pesticides.

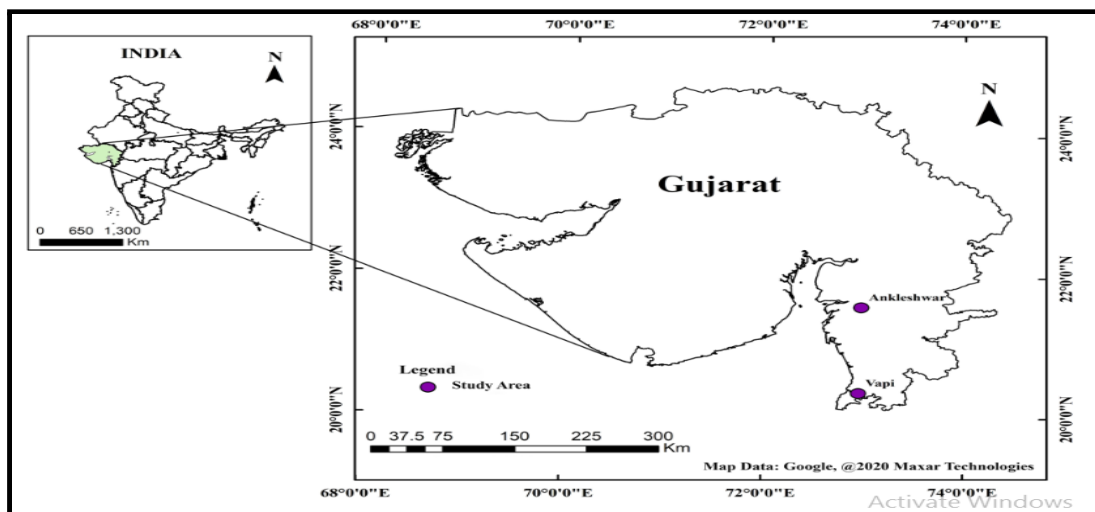


Figure 3. The locations of industrialized cities Ankleshwar in Gujarat, India.

1.2. Method: Air Quality Index (AQI)

The Air Quality Index (AQI) is used for reporting daily air quality. It tells you how clean or polluted your air is, and what associated health effects might be a concern for you. The AQI focuses on health effects you may experience within a few hours or days after breathing polluted air.

The automatic monitoring network AQI consists of the monitoring of eight major parameters (Figure 4).

AQI Category	AQI	PM ₁₀	PM _{2.5}	NO ₂	O ₃	CO	SO ₂
Good	0 - 50	0- 50	0 - 30	0 - 40	0 - 50	0 - 1.0	0 - 40
Satisfactory	51 - 100	51 - 100	31 - 60	41 - 80	51 - 100	1.1 - 2.0	41 - 80
Moderately polluted	101 - 200	101 - 250	61 - 90	81 - 180	101 - 168	2.1- 10	81 - 380
Poor	201 - 300	251 - 350	91 - 120	181 - 280	169 - 208	10.1 - 17	381 - 800
Very poor	301 - 400	351 - 430	121 - 250	281 - 400	209 - 748*	17.1 - 34	801 - 1600
Severe	401 - 500	430 +	250+	400+	748+*	34.1+	1600+

Figure 4. Breakpoints for AQI Scale 0–500 (all pollutants are in units of $\mu\text{g}/\text{m}^3$ and CO is expressed in units of mg/m^3)

to compute the index value, while the manual monitoring network AQI considers mainly PM10, SO₂, and NO₂ pollutants³⁹. Under the NAQI, the averaging time for pollutants such as PM2.5, PM10, NO₂, SO₂, Pb, and NH₃ is 24-h whereas, O₃ and CO have the averaging time of 1-h. Except for CO which is measured in mg/m³, all other seven pollutants are measured in $\mu\text{g}/\text{m}^3$.

1.3. Result

The five phases of lockdown (four lockdowns and one unlock-1.0) had different sets of rules and restrictions for the general public. Phase-1 of the nationwide lockdown lasted from March 25 to April 14, 2020, with complete restrictions on economic activities. During the second lockdown phase which lasted for 19 days starting from April 15 to May 3, various parts of the cities were color-coded into green, orange, and red zones based on the number of the COVID-19 positive cases; the red zones indicating rapidly rising cases had total lockdown, orange zones (moderately rising cases) were provided with some relaxation, and the green zone (low positive cases) had the least restrictions among them. The third phase lasted for 14 days (May 4–17, 2020), whereas, the fourth phase (labeled as the last period of the nation-wide lockdown with change from the green, orange and red zones to the containment zone and buffer zone) was extended from May 18–31, 2020. The unlock 1.0 (referred to in the study as ‘phase-5’) commenced on June 1, 2020, with several restrictions uplifted everywhere, except in the containment zones (Figure 5). The differences in the magnitude of restrictions imposed during various lockdown phases had an indirect impact on the fluctuation in the air pollutant level due to the restarting of several economic activities in the cities. The concentration values of six air pollutants (PM10, PM2.5, NO₂, O₃, CO, and SO₂) during the nationwide lockdown period in 2020 and for the similar period of 2019 were downloaded from the daily NAQI data portal available at cpcb.nic.in which is maintained by the Ministry of Environment, Forest and Climate Change, Government of India.

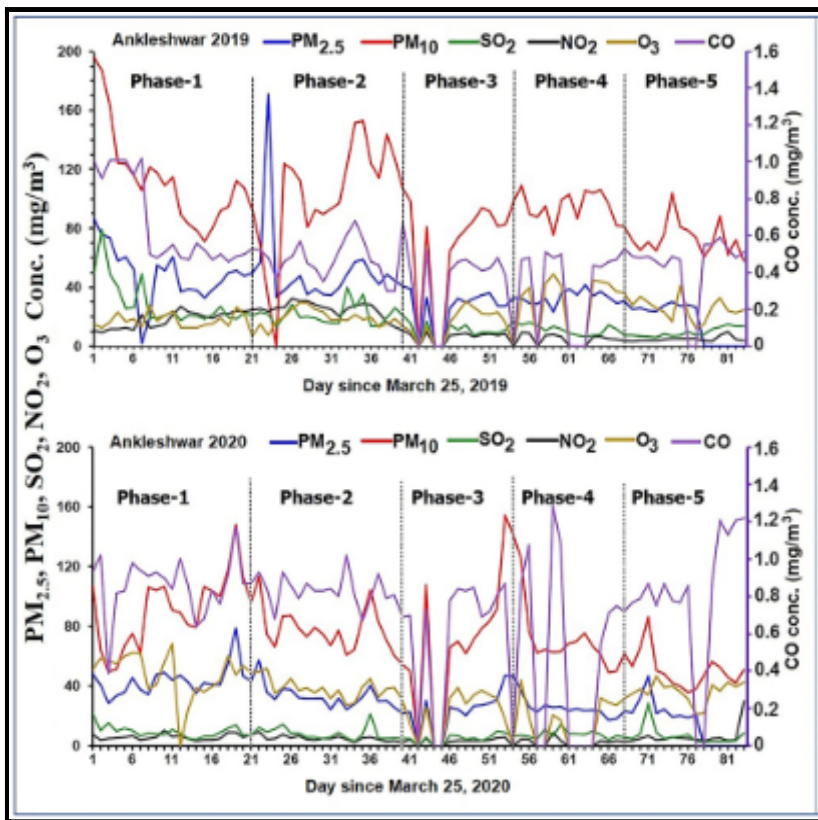


Figure 5. Mean concentrations of air pollutants from March 25 to June 15 for the years 2019 and 2020 for Ankleshwar, Gujarat, India.

Period	PM _{2.5}		PM ₁₀		SO ₂		O ₃		CO		NO ₂	
	Mean diff (%)	SD diff (%)	Mean diff (%)	SD diff (%)	Mean diff (%)	SD diff (%)	Mean diff (%)	SD diff (%)	Mean diff (%)	SD diff (%)	Mean diff (%)	SD diff (%)
Ankleshwar												
Phase-1	-10	-46	-19	-30	-67	-75	192	113	30	-35	-67	-67
Phase-2	-36	-74	-29	-50	-63	-38	98	20	74	-20	-80	-71
Phase-3	-6	131	5	231	-54	-51	44	35	84	100	-50	33
Phase-4	-26	-3	-27	67	-30	-16	-31	86	91	243	-37	5
Phase-5	-5	335	24	11	-28	123	44	-1	150	-99	27	35

Figure 6. Mean difference and standard deviation difference (rounded up for clarity) observed during different lockdown phases of 2020 in comparison to the same period in 2019 for Ankleshwar, Gujarat, India.

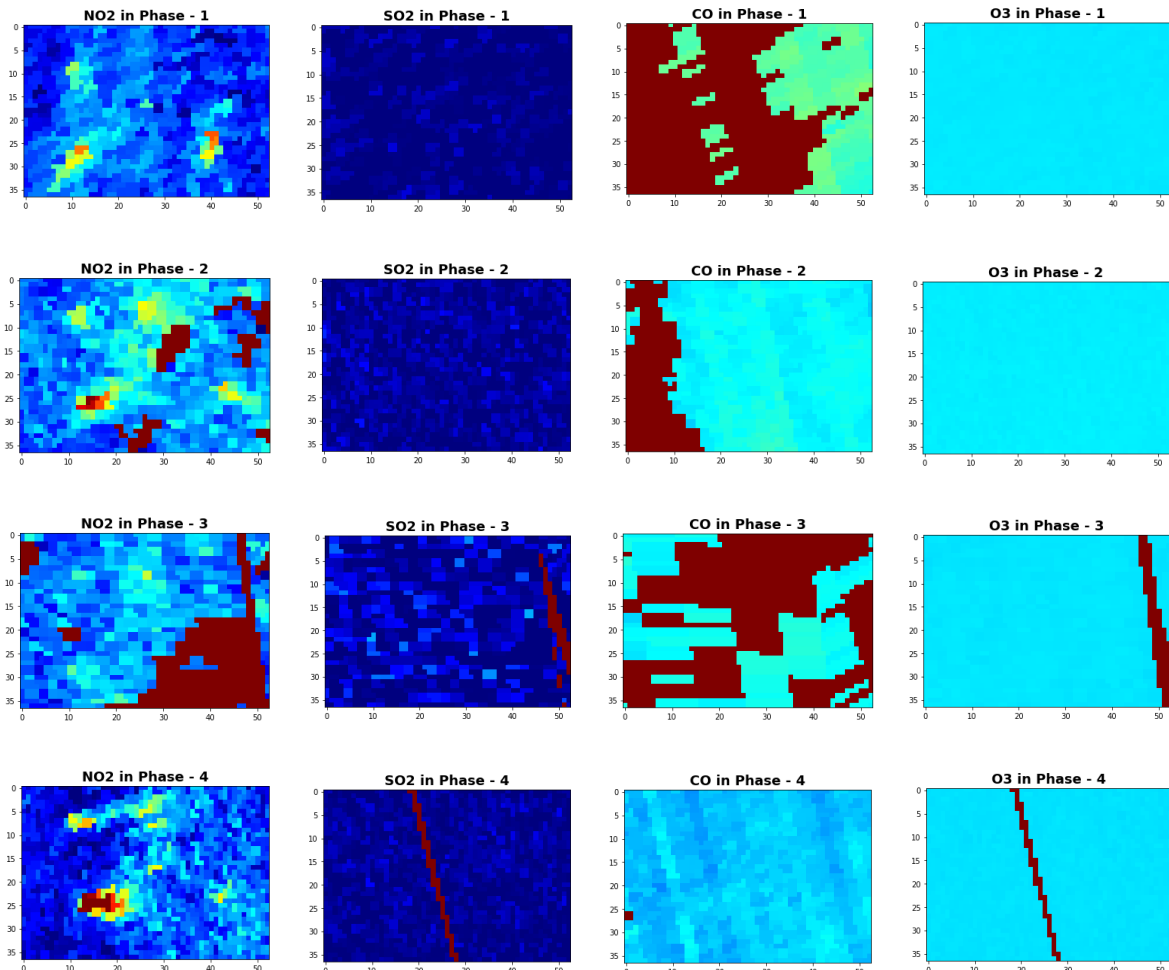
The Meta-analysis of continuous data was performed using descriptive and inferential statistical techniques to determine the number of variations (reduction or increase) in the air pollutant levels during the different phases, to calculate the mean differences (Figure 6). Additionally, the standard deviation was also computed to determine the fluctuation of air pollutants during different periods.

The mean distribution of air pollutants during lockdown for COVID-19 and a similar period in 2019 for Ankleshwar is shown in (Figure 6). In Ankleshwar, the maximum decline was observed in NO₂ (80%) during phase-2 O₃ increased by 192% and 310% in Ankleshwar during phase-1. SO₂ declined by - 67% during phase-1 and rose to - 28% during unlock 1.0 in Ankleshwar but it dropped to a maximum of 81% during phase-2. PM_{2.5} ranged between - 36 and - 5% during phase-2 and phase-5, respectively in Ankleshwar. PM₁₀ also showed a similar trend but it did not decline below 29% and 52% during phase-2 in Ankleshwar. CO continued to increase in Ankleshwar from 30% in phase-1 to 150% in phase-5 (unlock 1.0).

Pollutant	Phase 1 (Lockdown 1.0)				Phase 2 (Lockdown 2.0)				Phase 3 (Lockdown 3.0)				Phase 4 (Lockdown 4.0)				Phase 5 (Unlock 1.0)			
	Mean	Min	Max	SD	Mean	Min	Max	SD												
ANKLESWAR 2019																				
PM 2.5	48.670	1.870	86.410	18.750	50.731	33.470	171.000	30.138	31.881	25.780	38.800	3.995	32.943	23.070	41.660	4.751	26.482	23.870	30.060	2.076
PM 10	113.345	71.150	196.290	33.193	108.501	32.290	152.900	30.094	84.567	64.690	98.580	10.417	94.401	75.380	109.080	10.738	72.949	57.930	104.070	11.814
NO	18.015	9.230	26.670	5.690	24.689	10.610	32.590	5.892	8.139	6.680	9.710	0.823	6.732	3.790	9.340	1.762	4.882	3.130	9.890	1.748
SO ₂	28.995	17.500	79.250	15.707	21.488	13.370	39.670	7.089	12.310	7.550	16.990	3.354	10.843	6.400	16.220	3.246	9.448	6.140	14.870	2.990
CO	0.663	0.460	1.020	0.236	0.479	0.300	0.680	0.110	0.439	0.380	0.520	0.043	0.477	0.430	0.530	0.031	0.502	0.430	0.590	0.043
OZONE	17.113	6.920	27.880	5.245	19.184	7.640	29.740	5.582	20.302	10.090	30.680	6.317	41.095	34.490	48.970	4.418	25.217	11.990	41.370	7.538
ANKLESWAR 2020																				
PM 2.5	43.694	28.540	78.540	10.112	32.439	21.610	57.280	7.735	30.107	20.230	47.270	8.919	24.424	16.970	37.110	4.615	25.259	19.140	46.790	9.012
PM 10	91.413	49.380	148.190	24.285	77.031	54.560	113.200	14.617	88.775	50.010	154.230	33.151	68.518	49.130	125.690	18.244	50.338	35.800	86.550	12.659
NO	5.849	3.400	10.410	1.887	4.894	2.540	9.150	1.669	4.066	2.980	5.500	1.042	4.166	2.640	9.000	2.028	6.219	3.150	29.760	6.582
SO ₂	9.434	4.370	21.900	3.972	7.986	2.890	21.250	4.383	6.138	3.360	9.760	1.930	7.567	4.050	14.340	2.711	6.646	2.440	28.480	6.439
CO	0.861	0.390	1.170	0.157	0.826	0.670	1.020	0.088	0.782	0.690	0.870	0.067	0.880	0.540	1.290	0.249	1.251	0.750	5.380	1.252
OZONE	50.023	24.530	68.360	11.155	37.945	27.080	51.960	6.544	29.428	14.270	39.050	8.082	27.741	16.970	44.140	8.762	36.327	21.160	46.690	7.189

Figure 7. Variation air pollutant concentrations for pre-COVID19 (2019) and COVID19 (2020) years. All pollutants are in units of $\mu\text{g}/\text{m}^3$ and CO is expressed in units of mg/m^3 .

The variance in NO₂, SO₂, CO, and O₃ has also shown in (Figure 7) using TROPOMI or Tropospheric Monitoring Instrument, which is a sensor onboard Sentinel 5P. The dataset has been collected using the Sentinel EO hub browser.



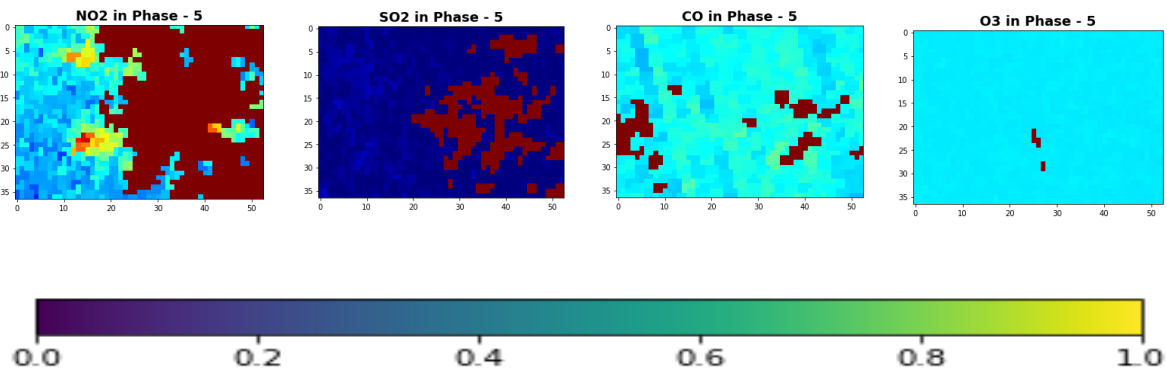


Figure 8. Variation air pollutant concentrations for COVID-19 (2020) years. All pollutants are in units of $\mu\text{g}/\text{m}^3$ and CO is expressed in units of mg/m^3 .

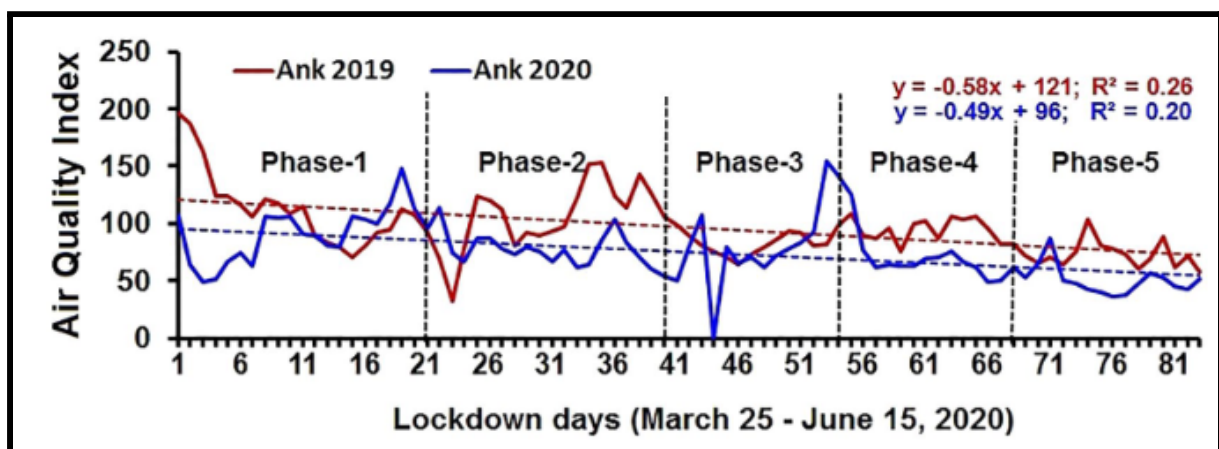


Figure 9. The AQI index for Ankleshwar, Gujarat, India.

This statistical analysis has been collected using the research paper case study.

2. Wildfire Events

Wildfires cause widespread destruction to a forest's natural ecosystems resulting in ecological, economic, and societal degradation. Wildfire smoke can irritate your lungs, cause inflammation, affect your immune system, and make you more prone to lung infections, including SARS-CoV-2, the virus that causes COVID-19. This session COVID-19 pandemic had become a nightmare for rain forests and natural resources, because of the COVID-19 pandemic, preparing for wildfires was a little different.

Existing research shows that the death rate from COVID-19 was significantly higher in polluted areas. In one study of over 3,000 counties in the United States, an increase of only 1 $\mu\text{g}/\text{m}^3$ of PM_{2.5} was associated with an 8% increase in the COVID-19 death rate. Another analysis of data from 2009-2018 in the state of Montana showed that higher PM_{2.5} concentrations from wildfire were associated with a 16-22% increase in influenza rates months later. Biologically, it makes sense that the increase in pollution from our current wildfires will cause a subsequent increase in COVID-19 rates. Even preparing for wildfire events and facing the wildfire event became hard during COVID-19. In April, citing concerns about social distancing and the respiratory danger of wildfire smoke, the U.S. Forest Service suspended a wildfire prevention method called controlled burns in several states. California, which had set aside billions to prepare for wildfires, had many projects put on hold after COVID-19's economic fallout forced the state to make significant budget cuts. Even due to social

distancing and pandemic, it was hard to control the wildfire and train new trainees because all the training sessions were going remotely.

2.1. Study-area

The Mendocino National Forest is located in the Coastal Mountain Range in north-western California and comprises 913,306 acres (3,696 km²) (Figure 10). It is the only national forest in the state of California without a major paved road entering it. The forest lies in parts of six counties. In descending order of forestland area, they are Lake, Glenn, Mendocino, Tehama, Trinity, and Colusa counties.

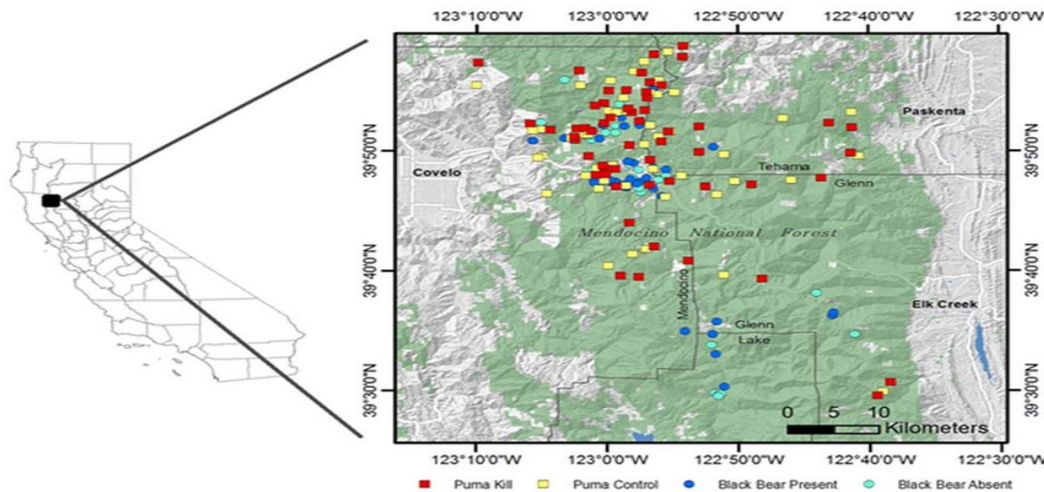


Figure 10. A map of the study area, in Mendocino National Forest. The study area is outlined by the thick black line, within the greater context of the North Coast Range and California.

2.2. Method: Normalized Burn Ratio (NBR)

It is the index that is used to measure burn severity by distinguishing areas that have been significantly altered in their spectral signature after a wildfire event. It is calculated using the energy intensity from the NIR and SWIR wavelength bands from the remotely sensed satellite imagery. The formula for NBR is similar to the Normalized Difference Vegetation Index (NDVI), which is based on the intensity of light coming from NIR and red wavelength bands. NBR uses the ratio between NIR and SWIR bands. High NBR values reflect areas covered with healthy vegetation, whereas low values indicate bare ground and recently burned areas. Near-zero values represent areas that are not affected by the fire event.

NBR for Sentinel 2 data is calculated as:

$$NBR = \frac{(NIR - SWIR)}{(NIR + SWIR)}$$

Burn Severity (dNBR)

Burn Severity is a term used to represent the degree to which an ecosystem is impacted by a wildfire event. It is estimated as the difference between pre-fire and post-fire NBR is derived from satellite images. To identify recently burned areas and differentiate them from bare soil and other non-vegetated areas, the difference

between pre-fire and post-fire NBR, also known as the delta Normalized Burn Ratio (dNBR) index is frequently used. Areas with high dNBR values correspond to a higher degree of damage or burn severity. In contrast, low dNBR values represent areas that are unaffected from the fire event or regions that have rebounded via the regrowth of plant species following a wildfire incident.

$$dNBR = NBR_{pre-fire} - NBR_{post-fire}$$

2.3. Result

The Landsat 8 Level 2 data used in this analysis has been acquired from the USGS Earth Explorer. For developing the post-fire assessment map, images obtained on 17 September 2020, i.e., master (Figure 12), and pre-fire assessment map 15 July 2020, i.e., slave has used (Figure 11).



Figure 11. Pre RGB composite band image of the study area, in Mendocino National Forest.



Figure 12. Post RGB composite band image of the study area, in Mendocino National Forest.

Once both pre-fire and post-fire images have been pre-processed, we merge them to form a new product containing pre-and post-fire NBR bands. As shown in (Figure 13).

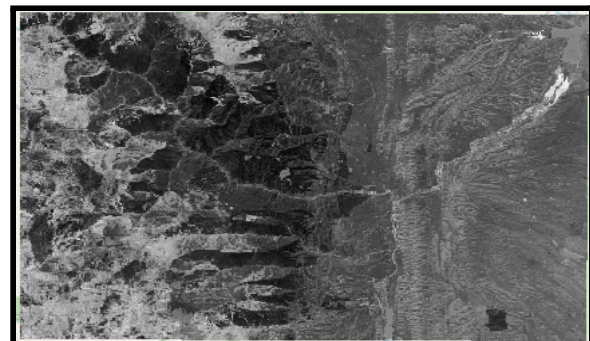
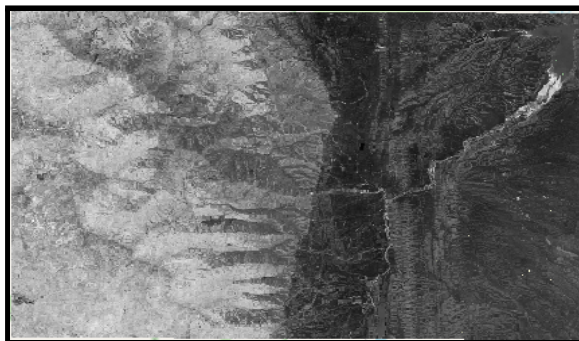


Figure 13. Comparing Pre NBR (left) and Post NBR (right) Landsat 8 L2 satellite images for the Mendocino National Forest, California.

The difference between both pre-fire and post-fire assessment maps is visual, the dark gray value in Post NBR represents the burn indexes. However, dNBR is an absolute measure of change, which can lead to issues in areas with low pre-fire vegetation cover, where the difference will be insignificant. To avoid such problems, we use the Relativized Burn Ratio (RBR):

$$RBR = \frac{(dNBR)}{(NBR_{pre-fire} + 1.001)}$$

For this dataset, the RBR values lie mostly between -0.25 and 0.6. Here is the change detection map of RBR in (Figure 14), which shows the burn areas.

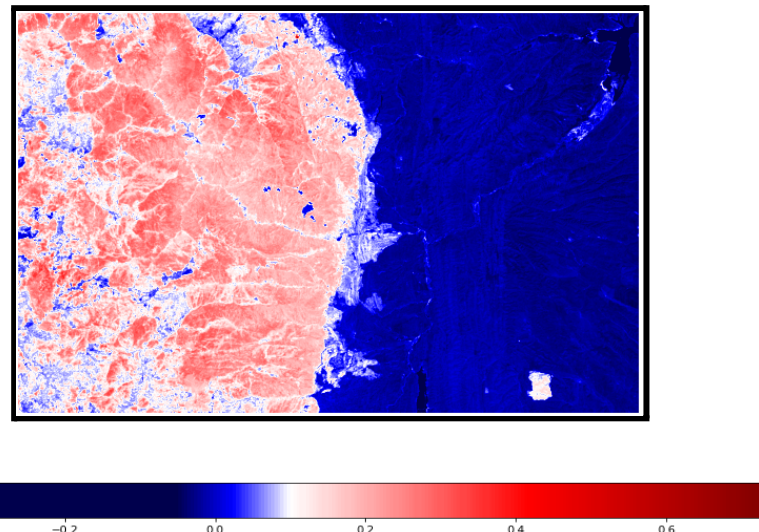


Figure 14. Change detection showing the fire-affected area in the Mendocino National Forest, California.

3. Deforestation

There is also a misperception for some places that nature is “getting a break” from humans during the COVID-19 pandemic. Instead, many rural areas in the tropics are facing increased pressure from land grabbing, deforestation, illegal mining, and wildlife poaching. People who have lost their employment in cities are returning to their rural homes, further increasing the pressure on natural resources while also increasing the risk of COVID-19 transmission to rural areas. Meanwhile, there were reports of increased deforestation in Asia, Africa, and Latin America. Illegal miners and loggers are encroaching on indigenous territories, which could expose remote indigenous communities to the virus. Areas that are economically dependent on tourism face reduced resources as tourism has come to a halt, resulting in a rise in bushmeat (wild meat) consumption in Africa. Meanwhile, illegal mining for gold and precious stones in Latin America and Africa is on the rise, as prices spike and protected areas are left unguarded.

Forest loss in Indonesia rose 50% in the first 20 weeks of 2020 compared to the same period in 2019, according to data from the Global Land Analysis and Discovery (GLAD) laboratory at the University of Maryland – which operates a global warning system for forest loss – and analyzed by Greenpeace. Analysis of the same data by WWF Germany found that in March alone, forest clearance in Indonesia was up 130% compared to the three-year average for March 2017 to 2019 with an estimated 130,000 hectares razed – the greatest recorded loss of any country that month. It is the starker example of a global trend that saw forest loss alerts rise significantly since the start of the pandemic across Asia, Africa, and Latin America.

3.1. Study-Area

Langkat Regency (Indonesian: Kabupaten Langkat) is the northernmost regency of North Sumatra (Figure 15). Its seat is Stabat. Its area is 6,263.29 km² and its population was 967,535 at the 2010 Census and 1,030,202 at the 2020 Census. Indonesia is the world's top palm oil producer and is heavily dependent on exports. Palm oil plantations have expanded from 3.6 million hectares in 2008 to 16.8 million in 2019, according to the Forest People's Programme.

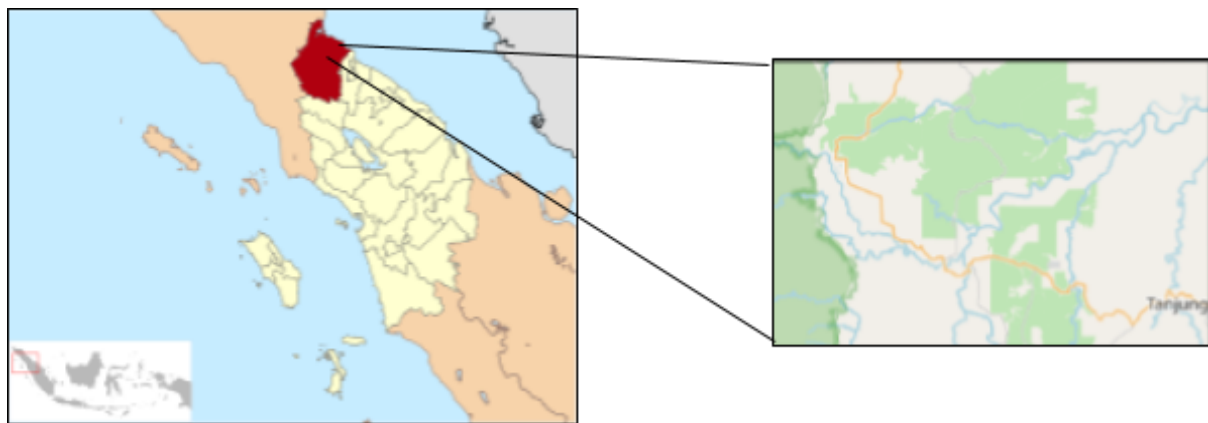


Figure 15. A map of the study area, in Tanjung Langkat Forest, Langkat regency, North Sumatra, Indonesia. The study area is outlined by the thick black line.

3.2. Method: Normalized Difference Vegetation Index (NDVI)

It is the index that is used to measure vegetation. It is calculated using the energy intensity from the NIR and red (which vegetation absorbs) wavelength bands from the remotely sensed satellite imagery. NDVI uses the ratio between NIR and Red bands. High NDVI values reflect areas covered with healthy vegetation, whereas low values indicate water area and close to zero areas indicate the urbanized area.

$$\text{NDVI} = \frac{(\text{NIR} - \text{Red})}{(\text{NIR} + \text{Red})}$$

3.3. Result

The Sentinel 2 Level 2B (L2B) data used in this analysis has been acquired from the Copernicus Open Access Hub. For developing the pre-vegetation assessment map, images obtained on 16 June 2019, i.e., master (Figure 17) and post-vegetation assessment map 6 October 2021, i.e., slave have been used (Figure 16).



Figure 16. Pre RGB composite band image of the study area, in Tanjung Langkat Forest.

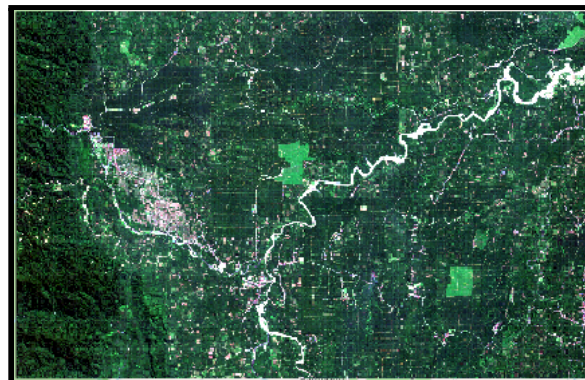


Figure 17. Post RGB composite band image of the study area, in Tanjung Langkat Forest.

Once both pre-NDVI and post-NDVI images have been pre-processed, we merge them to form a new product containing pre-and-post-NDVI bands. As shown in (Figure 18).

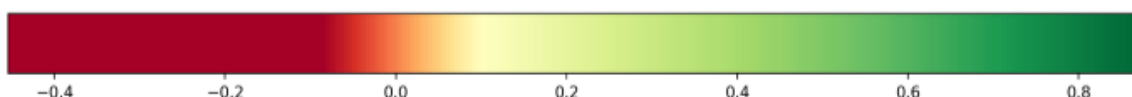
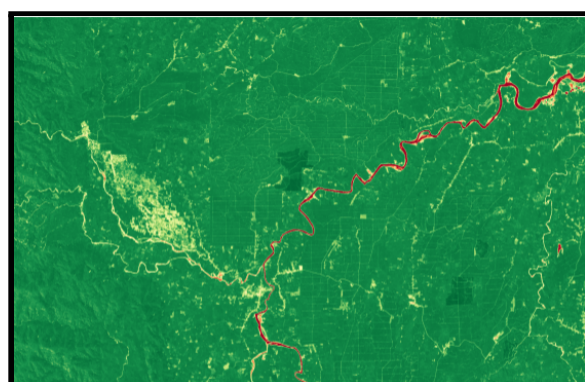


Figure 18. Comparing Pre NDVI (left) [2019] and Post NDVI (right)[2021] Sentinel-2 L2B satellite images for the Tanjung Langkat Forest.

Here for this dataset, the NDVI values lie mostly between 0.5 and 1.0. For calculating the absolute measure of change from 2019 to 2021, we calculate dNDVI, which shows the absolute difference,

$$dNDVI = NDVI_{pre} - NDVI_{post}$$

For this dataset, we perform the binary threshold on dNDVI between the range of [-0.10,0.05], and as the result, dNDVI represents the change in deforestation which lies mostly between 0.8 and 1.0. Here is the change detection map of dNDVI in (Figure 19) with blue color.

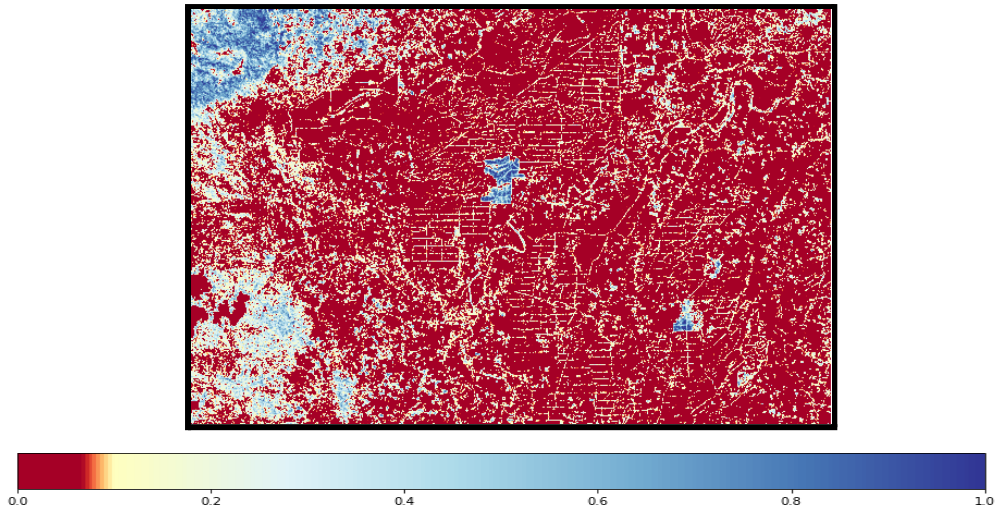


Figure 19. Change detection showing the deforested area in the Tanjung Langkat Forest.

4. Urban Growth

The remarkable growth of cities in recent decades has intensified a number of humanity's most pressing challenges. It has also presented many of the greatest opportunities to protect people, prosperity, and the planet. COVID-19 has laid bare – and indeed heightened – both these challenges and these opportunities.

With an estimated 90 percent of all reported COVID-19 cases, the urban area has become the epicenter of the pandemic. The size of their populations and their high level of global and local interconnectivity make them particularly vulnerable to the spread of the virus. This study shows that due to the COVID-19 pandemic there had been complete lockdown which led to the stop of transportation and mobility of people result in a decrement in urbanization.

4.1. Study-Area

Hong Kong, officially the Hong Kong Special Administrative Region of the People's Republic of China (HKSAR), is a metropolitan area and special administrative region of China on the eastern Pearl River Delta in South China. With over 7.5 million residents of various nationalities[e] in a 1,104-square-kilometre (426 sq mi) territory, Hong Kong is one of the most densely populated places in the world (Figure 20).

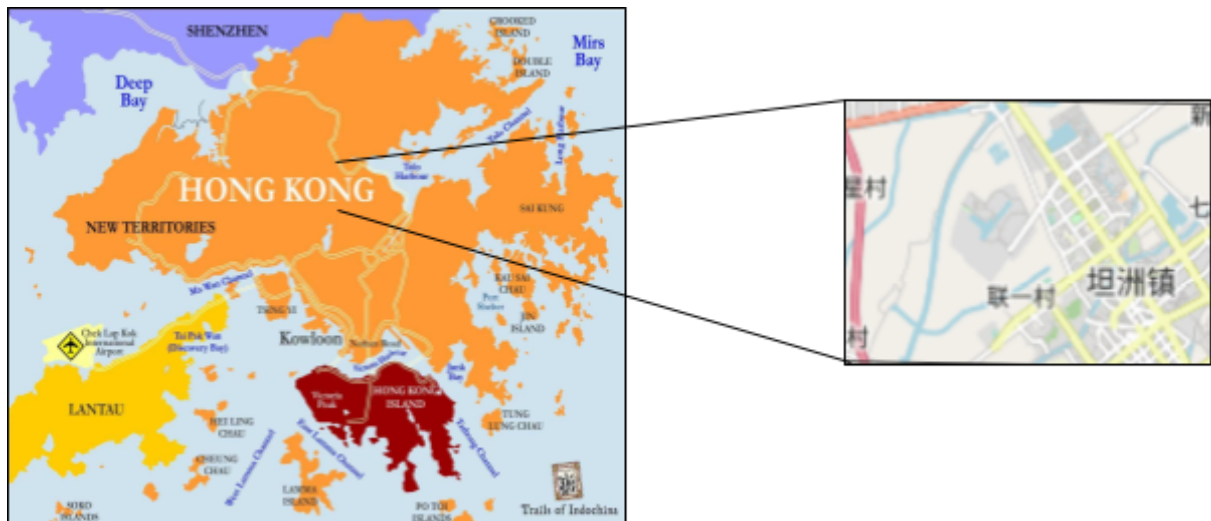


Figure 20. A map of the study area, in Hong Kong, China. The study area is outlined by the thick black line.

4.2. Method: Normalized Difference Build-up Index (NDBI)

The Normalized Difference Build-up Index (NDBI) highlights urban areas with higher reflectance in the shortwave infrared spectral range (SWIR). It is calculated using the energy intensity from the NIR and SWIR wavelength bands from the remotely sensed satellite imagery. NDBI uses the ratio between NIR and SWIR. The Normalized Difference Build-up Index value lies between -1 to +1. A negative value of NDBI represents water bodies whereas the higher value represents build-up areas. NDBI value for vegetation is low.

$$NDBI = \frac{(SWIR - NIR)}{(SWIR + NIR)}$$

Built-up Index (BU)

Build-up Index is the index for analysis of urban patterns using NDBI and NDVI. The built-up index is the binary image with only a higher positive value indicates built-up and barren thus, allows BU to map the built-up area automatically.

$$BU = NDBI - NDVI$$

4.3. Result

The Landsat 8 Level 2 data used in this analysis has been acquired from the USGS Earth Explorer. For developing the post-urban growth assessment map, images obtained on 20 February 2020, i.e., master (Figure 22) and pre-urban growth assessment on 20 January 2020, i.e., slave have been used (Figure 21).



Figure 21. Pre RGB composite band image of the study area, in Hong Kong, China.



Figure 22. Post RGB composite band image of the study area, in Hong Kong, China.

Once both pre-NDBI [2020] and post-NDBI [2021] images have been pre-processed, we merge them to form a new product containing pre-and-post-NDBI bands. As shown in (Figure 23). Here for this dataset, the NDBI values lie mostly between 0.05 and 1.0.

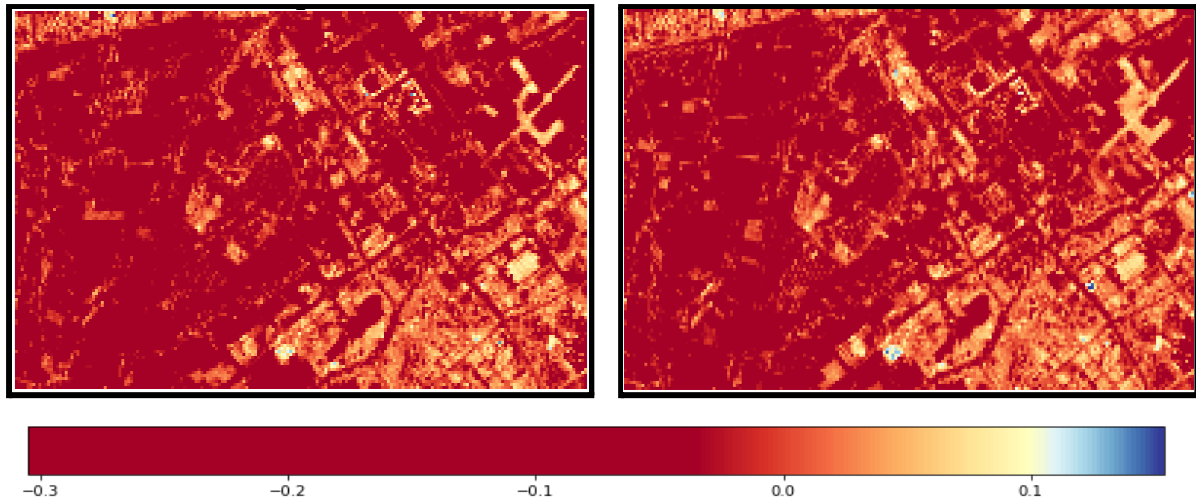


Figure 23. Comparing Pre NDBI (left) [2020] and Post NDBI (right)[2021] Landsat-8 2B satellite images for before Hong Kong, China.

On the other hand, once both pre-NDVI [2020] and post-NDVI [2021] images have been pre-processed, we merge them to form a new product containing pre-and-post-NDVI bands. As shown in (Figure 24). Here for this dataset, the NDVI values lie mostly between 0.2 and 1.0.

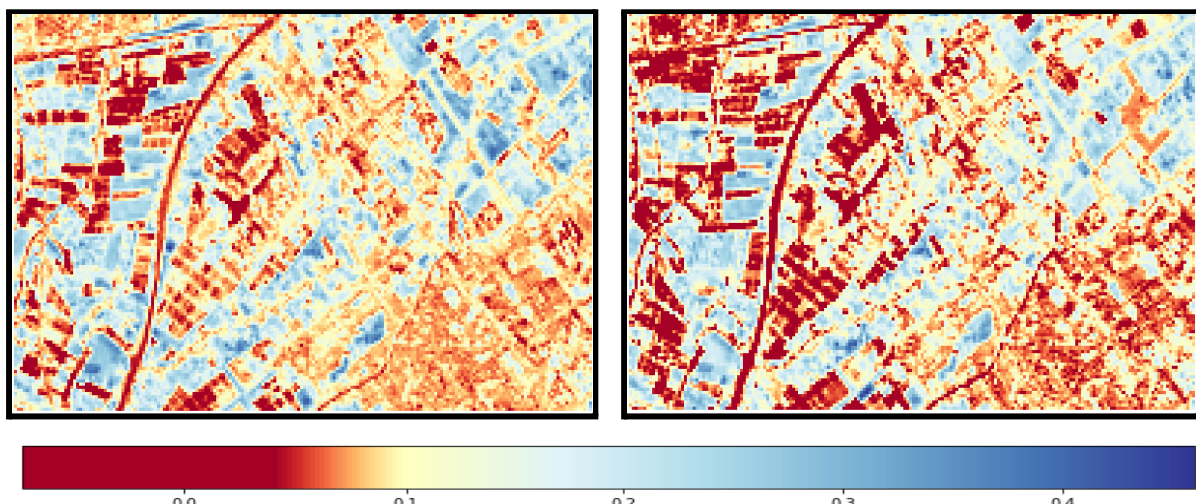


Figure 24. Comparing Pre NDVI (left) [2020] and Post NDVI (right) [2021] Landsat-8 2B satellite images for Hong Kong, China.

For the final result, the built-up areas have been extracted by the BU equation. As shown in (Figure 25), Here for this dataset, the BU values lie mostly between 0.2 and 1.0. The greater the value of a pixel in BU is, the higher is the possibility of the pixel being a built-up area.

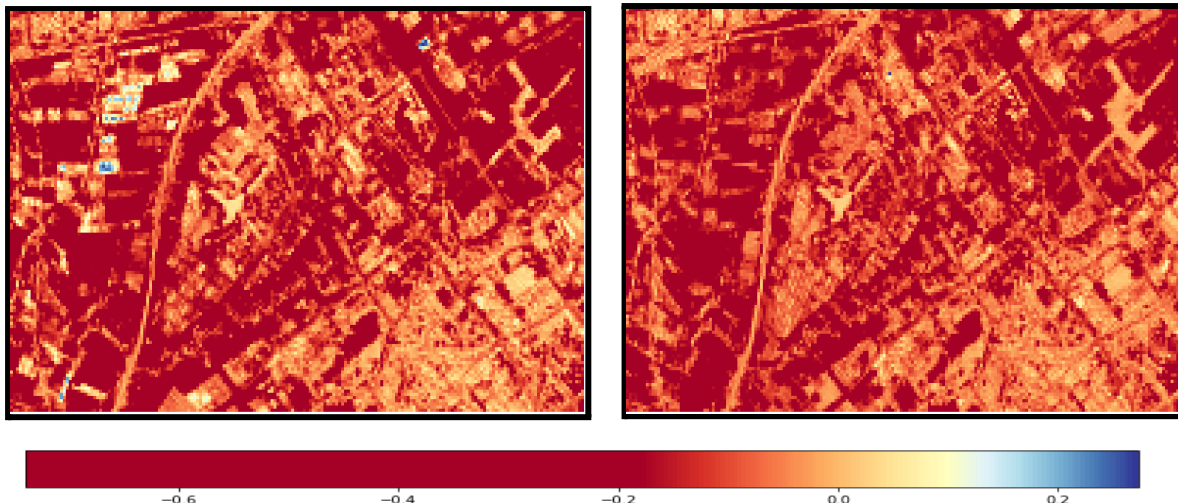


Figure 25. Comparing Pre BU (left) [2020] and Post BU (right) [2021] Landsat-8 2B satellite images for Hong Kong, China.

Conclusion

There have been several impacts of COVID-19 around the world. This study shows that the environmental changes caused by COVID-19 and societal response to it have both positive and negative effects. In some scenarios, it has shown positive changes, and somewhere it was negative too. Now coming to the positive result, there was huge declination in air pollution during COVID-19 the study shows it effectively. Air pollution has become a severe problem in various metropolitan cities and industrialized centers across the country. Incomplete combustion of fossil fuels by vehicles and industrial operations, and improper disposal of anthropogenic waste are the root causes of the rapid increases in air pollution. In March 2020, the COVID-19 pandemic led to a nationwide lockdown to control the spread of infection.

The total stretch of various phases of lockdown was 68 days. This long stretch of restrictions on economic activities provided an opportunity for improving Air quality. On the other hand, when we talk about negative impacts, Deforestation, wildfire events, and urbanization has taken the negative curve during this pandemic. This study shows the visual impact of wildfire around the world. due to social distancing and pandemic, it was hard to control the wildfire. There were many places where the army couldn't reach to help people and the wildfire smoke did also increase the number of cases of COVID-19. In the subject of deforestation, this study has taken the points from many research papers that there has been an opportunity for illegal forest cutting around Indonesia due to this COVID-19 lockdown. At the last when it comes to urbanization, there has been somewhere middle effect of COVID-19, because of travel restriction the industrialization had been put on hold in some places.

References

1. <https://reader.elsevier.com/reader/sd/pii/S0048969720335531?token=F8FF5FC8D9A837EC29591CEC9C8A454477E9E949A0E5242BEC943F4E4EE819B90F359545F86D8E5C9B2A3B4E0391FD38&originRegion=eu-west-1&originCreation=20210915045901>
2. https://www.researchgate.net/figure/A-map-of-the-study-area-in-Mendocino-National-Forest-The-study-area-is-outlined-by-the_fig4_263199893
3. <https://blogs.bmj.com/bmj/2020/09/25/california-wildfires-impact-of-air-pollution-during-the-COVID-19-pandemic/>
4. <https://www.nationalgeographic.com/science/article/COVID-19-complicates-already-dire-wildfire-season>
5. <https://www.conservation.org/stories/impact-of-COVID-19-on-nature>
6. <https://www.nature.com/articles/d41586-020-02341-1>
7. <https://www.climatechangenews.com/2020/08/18/forest-destruction-spiked-indonesia-coronavirus-lockdown/>
8. <https://news.mongabay.com/2020/07/COVID-19-lockdown-precipitates-deforestation-across-asia-and-south-america/>
9. <https://www.pnas.org/content/117/40/24609>
10. https://www.business-standard.com/article/economy-policy/COVID-19-impact-is-among-growing-complexities-cites-need-to-prepare-for-121061600553_1.html
11. <https://www.sciencedirect.com/science/article/pii/S0048969720359209>
12. https://www.unescap.org/sites/default/d8files/Aricle%205_Impact%20of%20COVID-19%20on%20Urban%20Mobility%20in%20Indian%20cities.pdf
13. <https://www.tandfonline.com/doi/pdf/10.1080/01431161.2010.481681>
14. <https://www.ncbi.nlm.nih.gov/pmc/articles/PMC7499053/>
15. <https://www.conserve-energy-future.com/urbanization-and-urban-growth.php>
16. <https://thecityfix.com/blog/will-COVID-19-affect-urban-planning-rogier-van-den-berg/>
17. <https://www.int-arch-photogramm-remote-sens-spatial-inf-sci.net/XLII-1-W2/43/2019/isprs-archives-XLII-1-W2-43-2019.pdf>
18. <https://www.nature.com/articles/s41598-021-83393-9.pdf>
19. <http://www.ieomsociety.org/gcc2019/papers/126.pdf>
20. <https://nirdeshthekumar.medium.com/monitoring-air-pollution-with-satellite-data-using-sentinel-5-p-in-python-2bbc6e1acef4>